Contributed paper

OPTO-ELECTRONICS REVIEW 9(4), 367–376 (2001)

Design considerations for InGaN/GaN/AlGaN quantum well lasers

T. CZYSZANOWSKI[1] and W. NAKWASKI*[1,2]

[1]Institute of Physics, Technical University of Łódź
219 Wólczańska Str., 93-005 Łódź, Poland
[2]Centre for High Technology Materials, University of New Mexico,
Albuquerque, NM 87131, USA

The rigorous optical model of diode lasers has been used to investigate an impact of various construction details of multi-quantum-well nitride lasers, as the number of quantum wells placed in active region, as well as designs of their waveguides and buffer layers located between the substrate and the laser structure, on room-temperature laser operation. The model is used to discuss some possible structure modifications to reduce lasing thresholds. Recommended design parameters have been found for each structure.

Keywords: optical model of diode lasers, nitride lasers, waveguide design, buffer layer design.

1. Introduction

Currently increasing number of technological centres are reporting manufacturing various designs of nitride lasers operating at room-temperature (RT). The designs differ from one another in many construction details therefore it is difficult to find their optimal structure. Seemingly their usability may be compared with the aid of their achievements, e.g. their RT thresholds, wall-plug efficiencies, differential external quantum efficiencies etc. But sometimes better performance characteristics follow mostly from better technology equipment, but not from a better design. Therefore the best way to optimise structures of nitride lasers is to use computer simulation of their operation. Such a simulation enables an investigation of a relative impact of many design details on performance characteristics of analysed laser construction to choose their really optimal design.

The main objective of this paper is therefore to use advance optical modelling of multi-layered semiconductor structures to investigate properties of the most advanced designs of nitride lasers and to optimise their structures for the RT operation.

2. The model

To investigate optical fields in complex multilayered structures of nitride lasers, the detailed model based on the approach reported by Bergmann and Casey [1] has been developed and presented in details in Ref. 2. Here, only the most crucial its elements are briefly explained. In semiconductor lasers, an optical gain is usually determined using the Fermi's Golden Rule and the envelope/Bloch function formalism for both the electron and hole wavefunctions. The total optical gain spectrum is then calculated as a sum of all possible band-to-band transitions between energy levels in the conduction band and both the light-hole and the heavy-hole valence bands, including the polarisation-dependent matrix element and the lineshape broadening effect. In our calculations, we have taken advantage of the results of the gain approach reported by Yeo *et al.* [3]. Because of a possible interwell inhomogeneity of carrier injection [4], a typical 5% concentration drop in successive quantum wells (QWs) has been assumed [5].

Two kinds of absorption have been considered in the simulation: the band-to-band absorption (within all semiconductor layers except the active ones) and the free-carrier absorption (within all semiconductor layers). The RT experimental absorption results reported by Muth *et al.* [6] have been interpolated to include in the model. Diffraction losses, i.e., unfavourable penetration of passive areas by the optical field, are included in the model by itself. Other than the described above possible absorption processes and all scattering losses are not included; they may be, however, considerably reduced using a precise technology. Also end losses, resulting from the emission of output beam, are omitted. The last loss mechanism is, however, practically the same for all TE radiation modes. Therefore it may be considered only as an additional factor increasing proportionally all lasing thresholds. Refractive index values have been derived from the results given in Ref. 1.

---

*e-mail: nakwaski@ck-sg.p.lodz.pl

3. Results of laser design optimisation

The optical model presented briefly in Section 2 will be used to optimise structures of nitride lasers (Fig. 1). In successive subsections, the most important laser design parameters, such as number of quantum wells, thickness of waveguide layers, thickness and compositions of both the buffer layers and the contact layers, have been discussed.

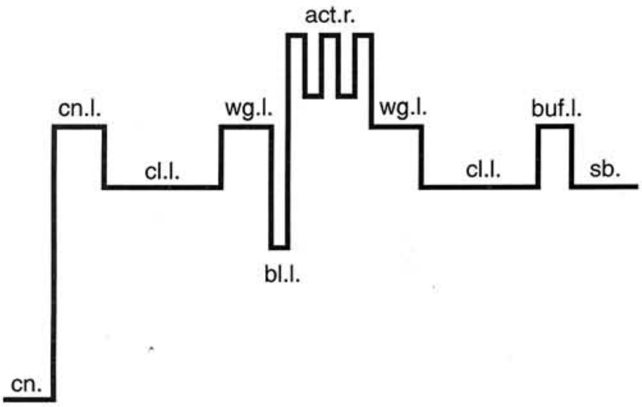

Fig. 1. Diagram of refractive index profile within layer structure of a typical design of nitride laser. cn. – contact, cn.l. – contact layer, cl.l. – cladding layer, wg.l. – waveguide layer, bl.l. – blocking layer, act.r – active region, buf.l. – buffer layer, sb. – substrate.

3.1. Number of quantum wells

The number N_{QW} of quantum wells in a laser active region is one of the most crucial structure parameters in diode laser designing. Recommended value of N_{QW} has been found to be proportional to total optical losses within the resonator [7]. Therefore, an increase in technological maturity, which is followed by improving layer homogenity (reduction of absorption) and interface smoothness (reduction of scattering), is expected to cause a steadily decreasing optimal number N_{OPT} of quantum wells, for which a minimal threshold is obtained.

We have examined 14 advanced structures of nitride lasers shown in Fig. 2. For five structures exhibiting the lowest RT thresholds, plots of RT threshold carrier concentration n_{th} versus N_{QW} are depicted in Fig. 3. As one can see, determined n_{th} values are more than one order of magnitude higher than analogous values known for conventional, i.e., arsenide and phosphide, lasers. Besides, optimal numbers N_{OPT} of QWs (ensuring the lowest n_{th} values) are surprisingly high. For structures under consideration they range from 10 up to 15 whereas, in conventional diode lasers, usually the single-quantum-well ($N_{QW} = 1$) active region enables obtaining the lowest threshold. It is also interesting to compare N_{OPT} with the numbers N_{QW} of quantum wells used in actually reported structures of nitride lasers (Table 1). Only Kimura *et al.* [8] (Pioneer 1 laser) chose an optimal number of QWs. All other designers applied too few quantum wells, distinctly below the N_{OPT} value.

Table 1. Designed (N_{QW}) and recommended (N_{OPT}) number of quantum wells.

Laser	Ref.	N_{QW}	N_{OPT}
Fujitsu 1	10	3	11
Fujitsu 2	11	5	13
Fujitsu 3	12	5	13
Nichia 1	13	3	13
Nichia 2	14	2	11
Nichia 3	15	4	12
Nichia 4	16	3	10
Nichia 5	17	4	14
Pioneer 1	8	10	10
Pioneer 2	18	5	13
Sony	19	4	12
Xerox 1	20	10	15
Xerox 2	21	10	14
Xerox 3	22	5	11

3.2. Waveguide design

Let us now consider the influence of the width d_{wav} of waveguide layers on RT laser threshold properties. To obtain high values of confinement factor Γ_{QW} (describing overlapping of carriers within active layer QWs and an optical field) as well as low threshold carrier concentrations n_{th}, d_{wav} should not be too thin since then the optical field will penetrate both the n- and the p-type claddings to an unaccepted extent and suffers from losses. On the other hand, it should not be too thick either, since then the smaller part of the field will interact with carriers inside the active region. Therefore there should exist an optimal waveguide width for each structure. Plots of Γ_{QW} versus d_{wav} for five laser designs are shown in Fig. 4. Analogous plots of threshold carrier concentration are presented in Fig. 5. As one can see, some laser structures are relatively less sensitive to the waveguide design than others. It concerns especially laser constructions for which n_{th} versus d_{wav} plots are depicted in Fig. 5(c), in particular the Pioneer2 design reported by Kimura *et al.* [8] and also the Fujitsu1 design reported by Kuramata *et al.* [15]. Values of optimal waveguide widths to obtain the highest value of Γ_{QW} as well as those for minimal n_{th} are shown in Table 2. Surprisingly only Bour *et al.* [10] in their Xerox1 laser and Kimura *et al.* [8] in their Pioneer2 laser chose waveguide width close to its optimal value.

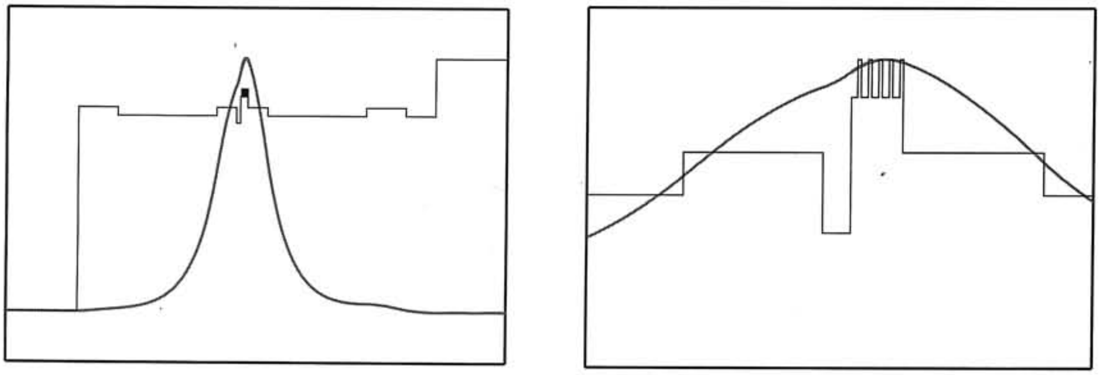

Fujitsu 1 (5 QWs)

(a)

Fujitsu 1 (5 QWs)

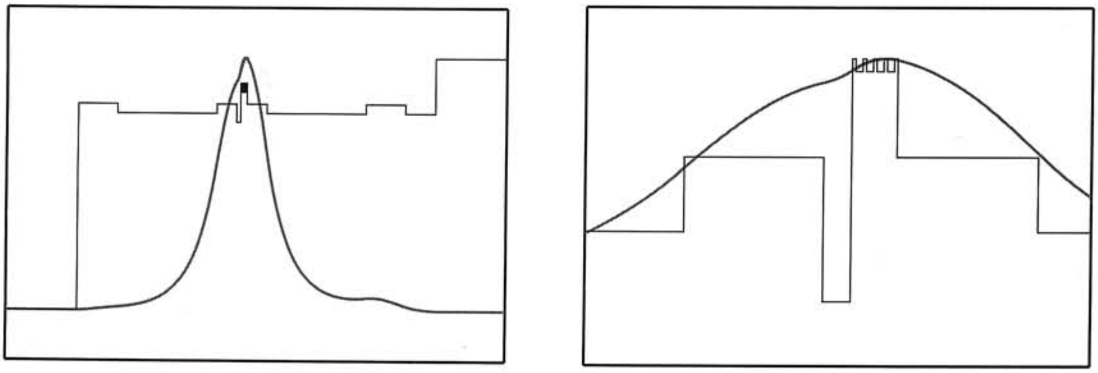

Fujitsu 2 (5 QWs)

(b)

Fujitsu 2 (5 QWs)

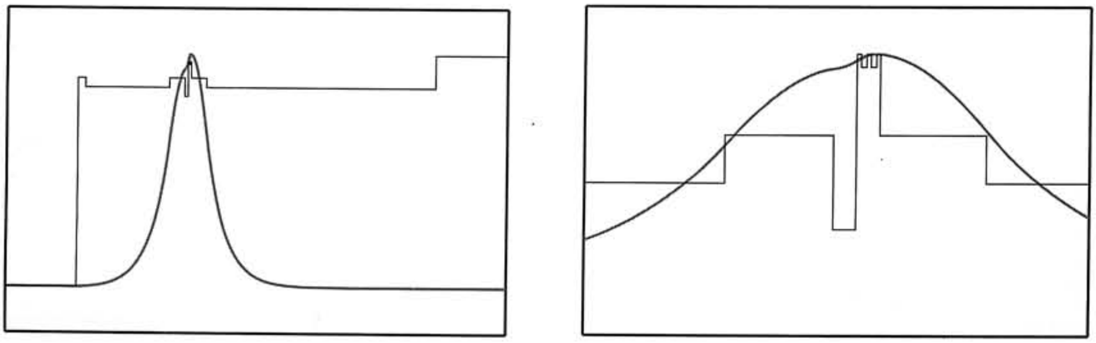

Fujitsu 3 (3 QWs)

(c)

Fujitsu 3 (3 QWs)

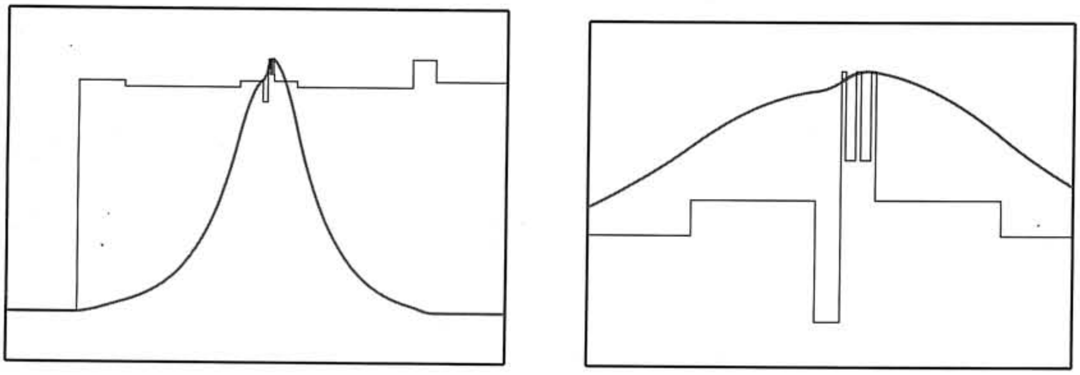

Nichia 1 (3 QWs)

(d)

Nichia 1 (3 QWs)

Fig. 2

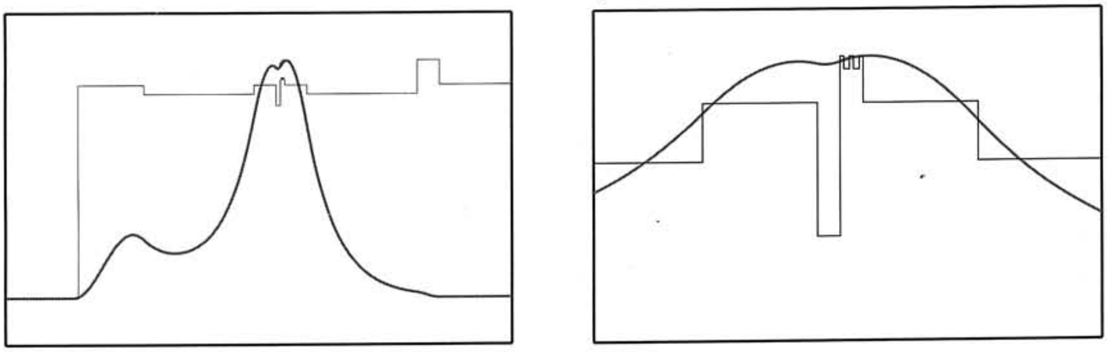

Nichia 2 (3 QWs) (e) Nichia 2 (3 QWs)

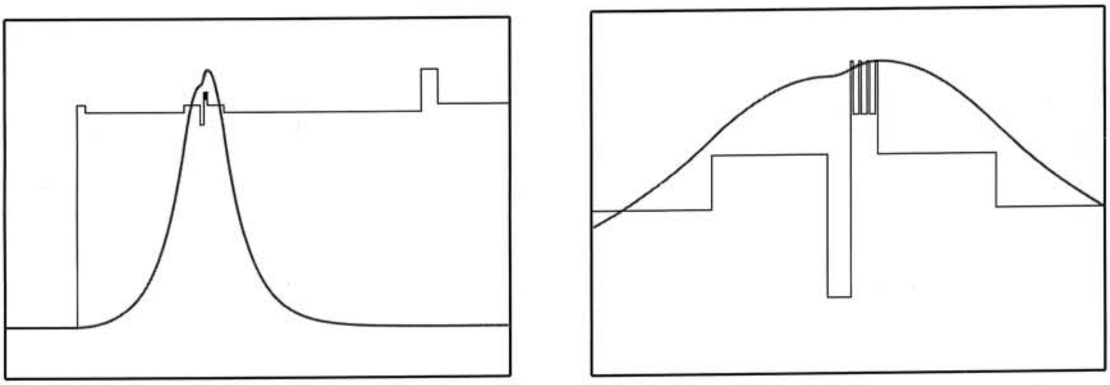

Nichia 3 (4 QWs) (f) Nichia 3 (4 QWs)

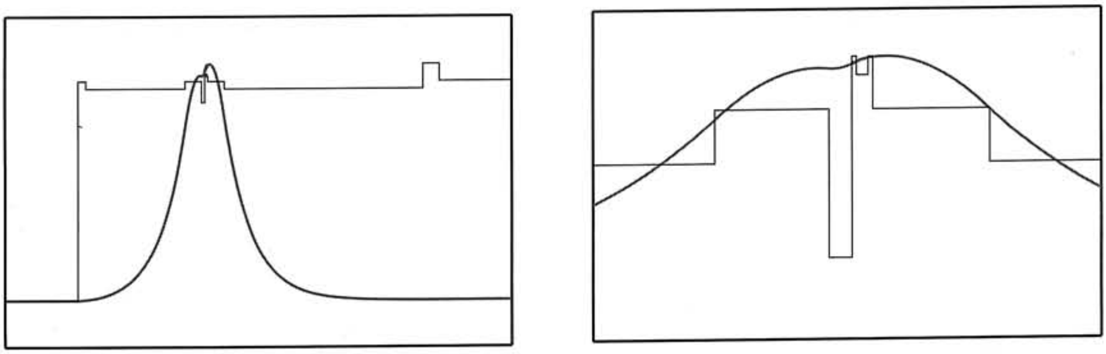

Nichia 4 (2 QWs) (g) Nichia 4 (2 QWs)

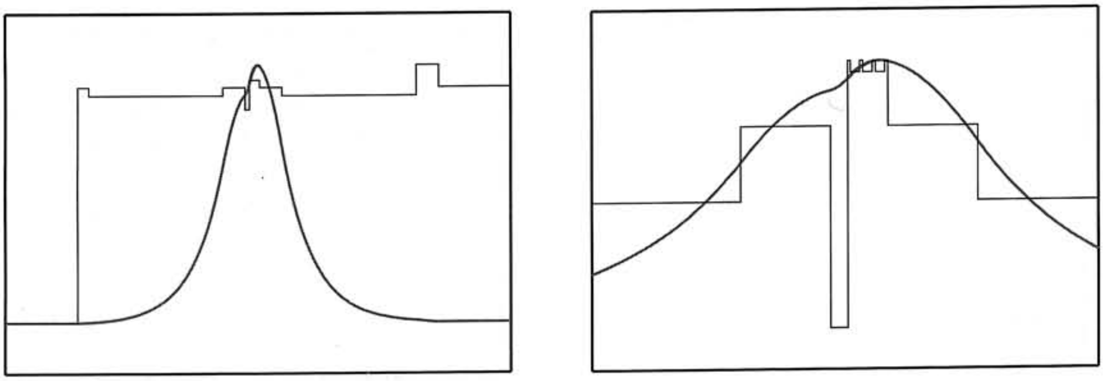

Nichia 5 (4 QWs) (h) Nichia 5 (4 QWs)

Fig. 2 (*continued*)

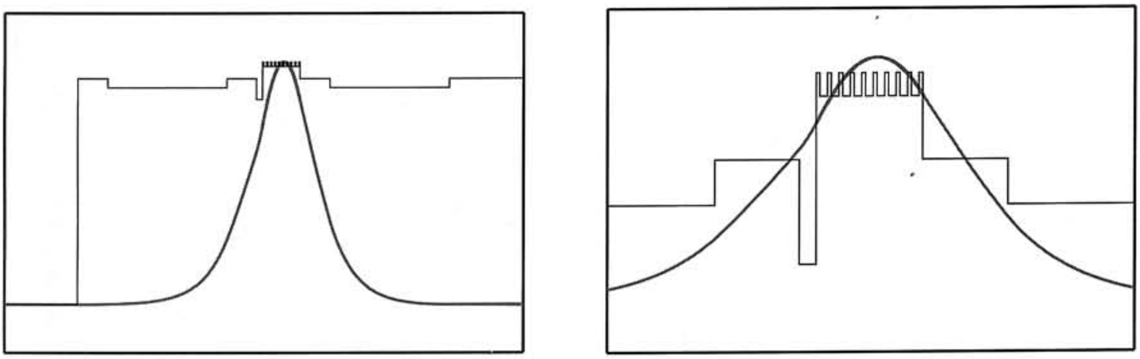

Pioneer 1 (10 QWs) (i) Pioneer 1 (10 QWs)

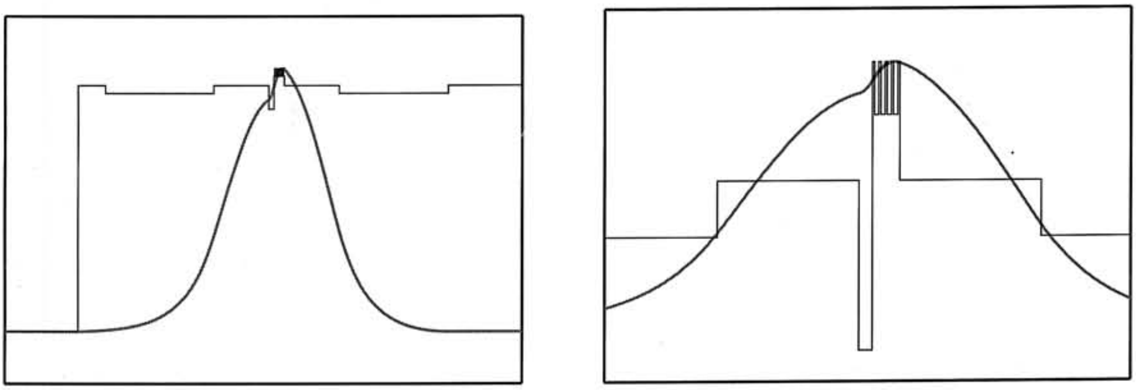

Pioneer 2 (5 QWs) (j) Pioneer 2 (5 QWs)

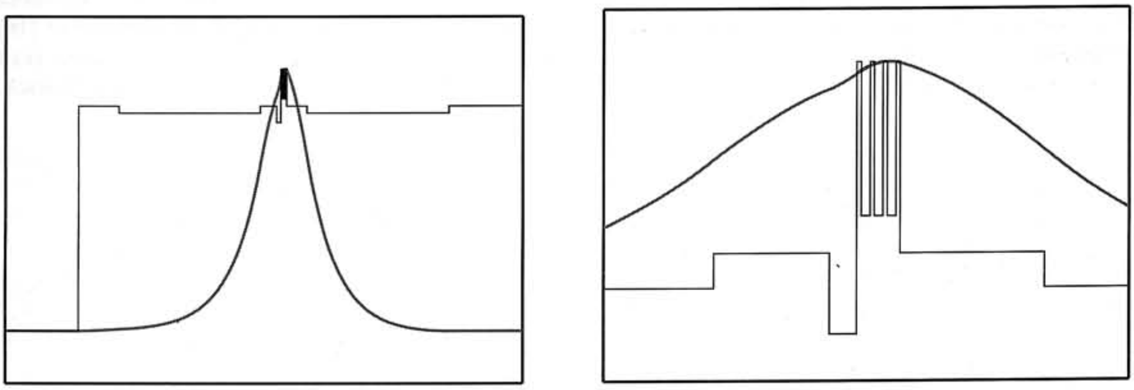

Sony (4 QWs) (k) Sony (4 QWs)

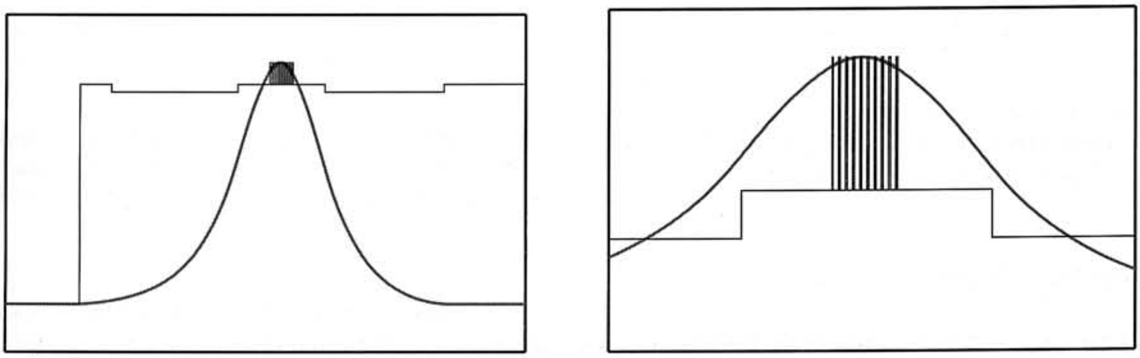

Xerox 1 (10 QWs) (l) Xerox 1 (10 QWs)

Fig. 2 (*continued*)

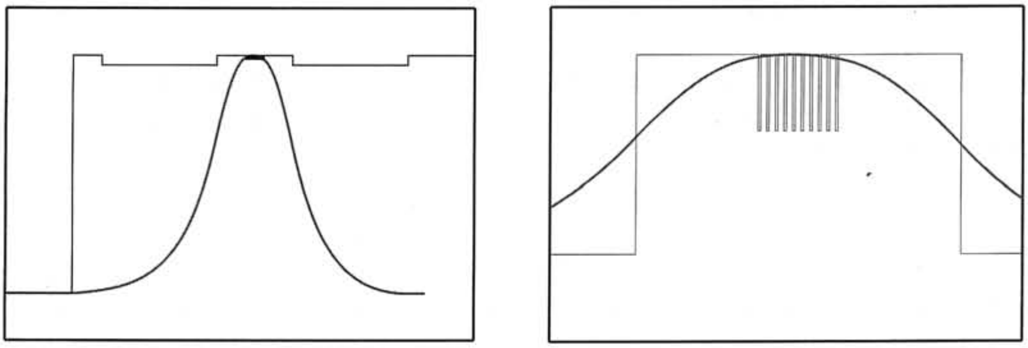

Xerox 2 (10 QWs) (m) Xerox 2 (10 QWs)

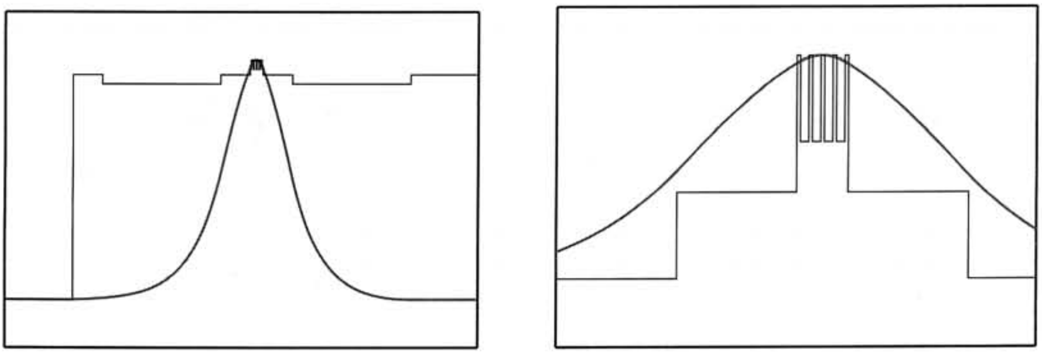

Xerox 3 (5 QWs) (n) Xerox 3 (5 QWs)

Fig. 2. Layer structures, refractive index changes and intensity profiles of the fundamental mode plotted for nitride lasers reported by: (a) Kuramata *et al.* [10] (Fujitsu1 laser), (b) Domen *et al.* [11] (Fujitsu2 laser), (c) Kuramata *et al.* [12] (Fujitsu3 laser), (d) Nakamura *et al.* [13] (Nichia1 laser), (e) Nakamura *et al.* [14] (Nichia2 laser), (f) Nakamura *et al.* [15] (Nichia3 laser), (g) Nakamura *et al.* [16] (Nichia4 laser), (h) Nakamura *et al.* [17] (Nichia5 laser), (i) Kimura *et al.* [8] (Pioneer1 laser), (j) Miyachi *et al.* [18] (Pioneer2 laser), (k) Kobayashi *et al.* [19] (Sony), (l) Kneissl *et al.* [20] (Xerox1 laser), (m) Bour *et al.* [21] (Xerox2 laser), (n) Bour *et al.* [22] (Xerox3 laser).

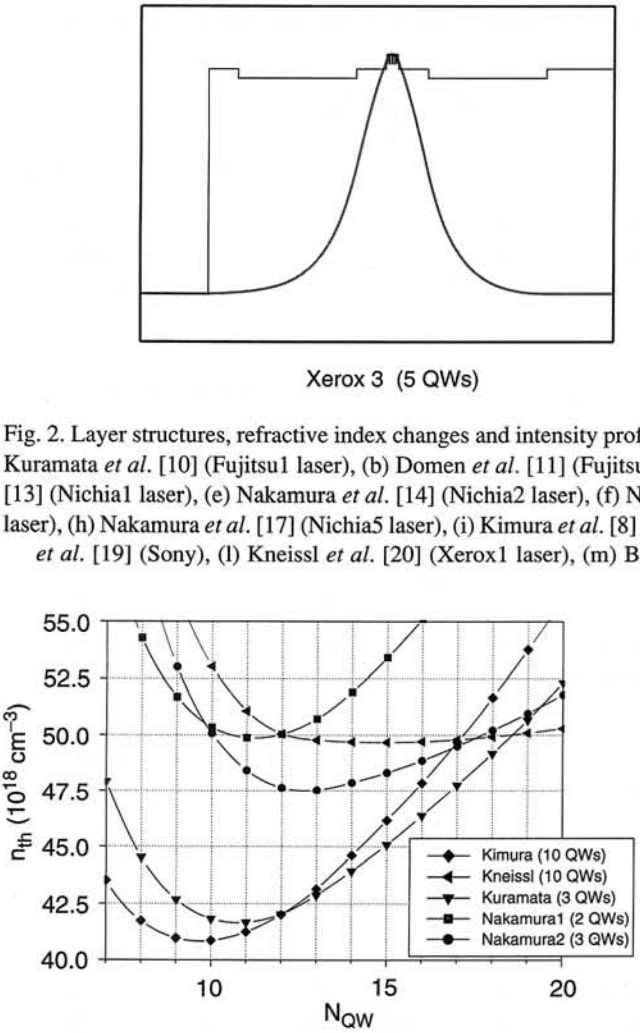

Fig. 3. RT threshold carrier concentration n_{th} (determined for nitride laser structures exhibiting the lowest n_{th}) versus the number N_{QW} of their active-layer quantum wells.

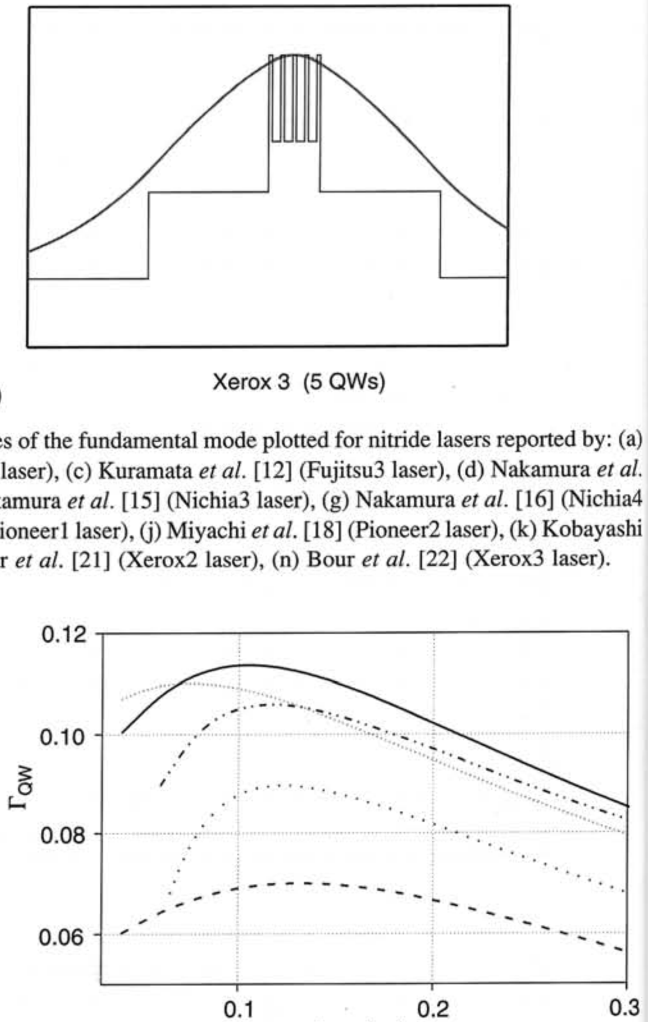

Fig. 4. The RT confinement Γ_{QW} factor versus the waveguide layer width for the lowest-threshold nitride lasers: (solid line) Nichia 3, (dot) Pioneer 1, (dash dot dot) Fujitsu 3, (short dash) Fujistu 2, (dash) Sony.

3.3. Buffer layer designs

An impact of the width d_{buff} and mole fraction x_{buff} of buffer layers (see Fig. 1) on RT lasing threshold as well as active region confinement factor has been also examined. Compositions and thicknesses of buffer layers are chosen mostly from technological point of view. But they may surprisingly influence on operation of nitride lasers to a considerably extent. They may create additional competitive waveguide located far from active regions and influencing efficiency of an energy exchange between carriers and the

Table 2. Designed (d_{wav}) and recommended widths of waveguide layer ensuring the lowest threshold [$d_{OPT}(n_{th})$] and the highest active region confinement factor [$d_{OPT}(\Gamma_{QWs})$].

Laser	Ref.	d_{wav}	$d_{opt}(n_{th})$	$d_{wav}(\Gamma_{QWs})$
Fujitsu1	10	0.1	0.16	0.12
Fujitsu2	11	0.1	0.16	0.12
Fujistu3	12	0.1	0.15	0.10
Nichia1	13	0.1	0.13	0.14
Nichia2	14	0.1	0.15	0.12
Nichia3	15	0.1	0.14	0.10
Nichia4	16	0.1	0.18	0.13
Nichia5	17	0.1	0.16	0.12
Pioneer1	8	0.1	0.11	0.03
Pioneer2	8	0.2	0.12	0.08
Sony	19	0.08/0.1	0.17/0.19	0.14/0.16
Xerox1	20	0.1	0.15	0.05
Xerox2	21	0.1	0.11	0.08
Xerox3	22	0.1	0.13	0.07

optical field. This may enhance migration of radiation that may be followed by unwanted modification or even transformation of radiation modes.

Plots of Γ_{QWs} versus d_{buff} and x_{buff} are shown in Fig. 6 and Fig. 7, respectively. Γ_{QW} changes observed in Fig. 6 follow from a creation of a competitive buffer waveguide of equal or even higher refractive index than that in an active layer. Then, mode modification or even mode transformation occurs which results in increasing penetration buffer layers by optical field at the expense of active layers. Both processes have been described in Ref. 9. Similar process may be observed in Fig. 7 as a result of changing buffer layer compositions. The refraction index of $In_xGa_{1-x}N$ is the highest for the InN mole fraction ranging from 0.05 to 0.10. Recommended values of buffer layer widths and their InN mole fraction are listed in Table 3. This time all considered laser designs are in agreement with our optimisation suggestions.

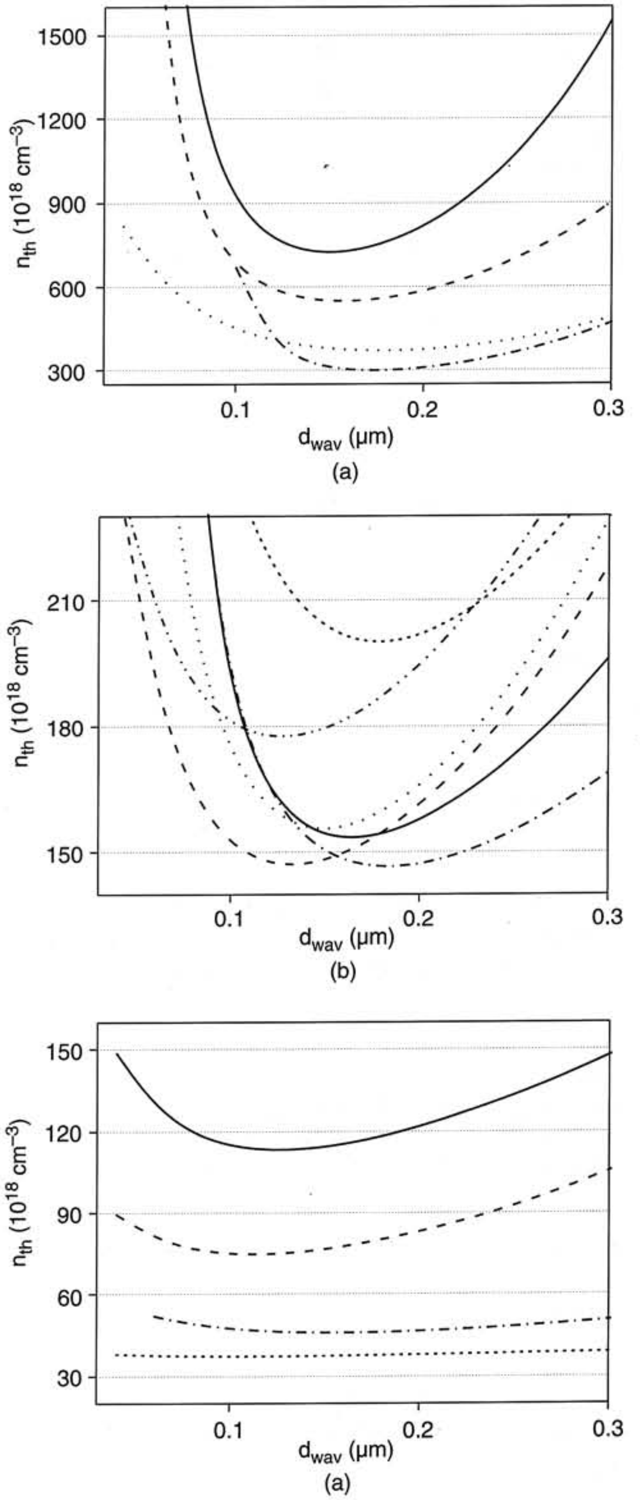

Fig. 5. The RT threshold concentration n_{th} versus the waveguide layer width for: (a) (solid line) Nichia2, (dash) Nichia1, (dot) Sony, (dash dot) Nichia5; (b) (dash) Nichia4, (dash dot dot) Pioneer1, (dot) Fujitsu1, (solid line) Fujitsu2, (dash) Nichia3, (dash dot) Fujitsu3; (c) (solid line) Xerox2, (dash) Xerox1, (dash dot) Xerox3, (short dash) Pioneer2.

3.4. Contact layers designs

In Figs. 6 and 7, an influence of a possible n-type contact layer (located between contact and cladding layer), (see Fig. 1) is also shown as "cn.l."-curves. Their impact has been proved to be less essential than that of buffer layers. Nevertheless, in detail designing of nitride lasers, optimisation of those layers should be also included. As one can see, the changes of buffer widths cause much deeper minimum in the p-type buffer layer case than in the n-type contact-layer case. The above is connected with lower value of refractive index in the p-type contact, comparing to the n-type contact, bordering on buffer layer. Therefore mode is better confined in an n-type part of structure. Increasing

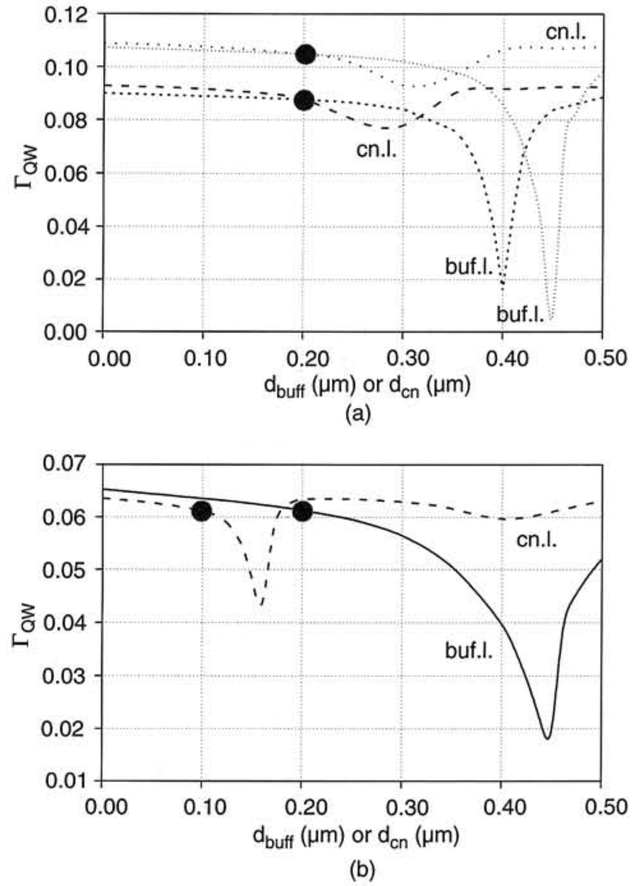

Fig. 6. The RT confinement Γ_{QW} factor versus the width d_{buff} of the buffer layer (buf.l. curves) or the d_{cn} width of the contact layer (cn.l. curves) for: (a) Fujitsu1 (dot), Fujitsu2 (dash), (b) Nichia1. Circles correspond to designed widths.

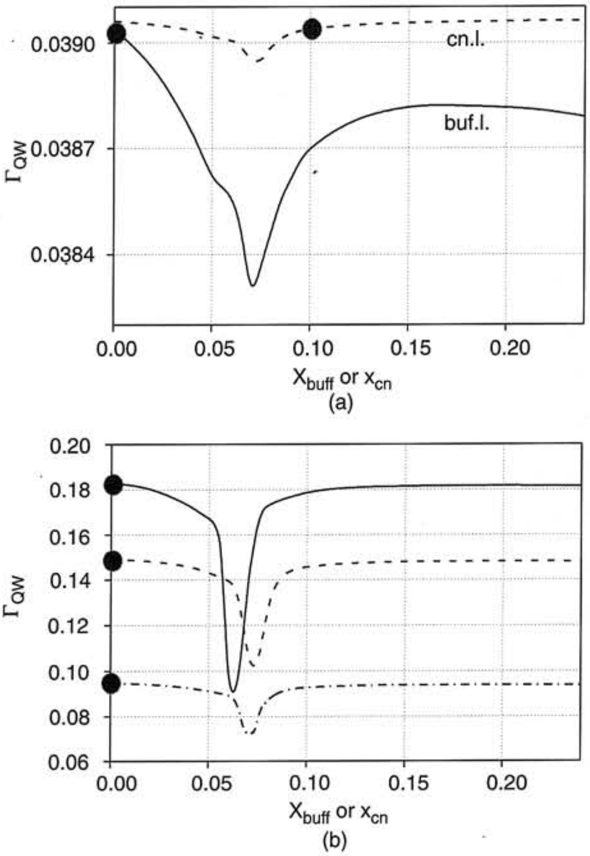

Fig. 7. The RT confinement Γ_{QW} factor versus the mole fraction x_{buff} of the buffer layer (buf.l. curves) or the x_{cn} mole fraction of the contact layer (cn.l. curves) for: (a) Nichia3, (b) Xerox2 (solid), Xerox3 (dash), Pioneer2 (dash dot). Circles correspond to designed mole fractions.

Table 3. Designed (d_{buff}) and recommended ranges of contact layers/buffer layer widths ensuring the lowest threshold (d_{OPT}) and designed (x_{buff}) and recommended ranges of contact layers/buffer layer mole fraction ensuring the lowest threshold (x_{OPT}). Parameters before backslash correspond to contact layer and behind to buffer layer. In case of lack of the backslash parameters describe the buffer layer only. Description 0-0.02; 0.06-0.14 means two regions ranged from 0 to 0.02 and from 0.06 to 0.14 ensuring the lowest threshold.

Laser	Ref.	d_{buff}	d_{OPT}	x_{buff}	x_{OPT}
Fujitsu1	10	0.2/0.2	0–0.3/0–0.15	0/0	0–0.02; 0.06–0.14 /0–0.01; 0.04–0.22
Fujitsu2	11	0.2/0.2	0–0.25/0–0.15; 0.4–0.5	0/0	0–0.01; 0.06–0.12/0–0.01; 0.04–0.18
Fujitsu3	12	0.05	0–0.25	0	0–0.24
Nichia1	13	0.3/0.1	0–0.15; 0.43–0.5/0–0.11; 0.18–0.34	0/0.05	0–0.06; 0.09–0.24/0–0.06; 0.1–0.24
Nichia2	14	0.05/0.1	0–0.15/0–0.5	0/0.1	0–0.24/0–0.24
Nichia3	15	0.05/0.1	0–0.25/0–0.35	0/0.1	0–0.24/0–0.24
Nichia4	16	0.2/0.1	0–0.18/0–0.1; 0.25–0.35	0/0.05	0–0.02; 0.2–0.24/0–0.05; 0.13–0.24
Nichia5	17	0.05/0.1	0–0.15/0–0.5	0/0.1	0–0.24/0–0.24
Pioneer1	8	0.1	0–0.35	0	0–0.04; 0.09–0.24
Pioneer2	18	0.1	0–0.5	0	0–0.24
Sony	19	0.2	0–0.18; 0.4–0.5	0	0–0.2; 0.04–0.14
Xerox1	20	0.1	0–0.3	0	0–0.08; 0.15–0.24
Xerox2	21	0.1	0–0.22	0	0–0.02; 0.1–0.25
Xerox3	22	0.1	0–0.15; 0.4–0.5	0	0–0.04; 0.1–0.25

width of the contact layer, which is characterised by equal or higher refractive index than active region, causes mode migration to this layer. Competitive waveguide is created and the mode modification occurs. Analogous processes have been reported in Ref. 9. Similar behaviour has been observed in mole fraction modification case. The refraction index becomes the highest for the InN mole fraction value in the range 0.05–0.10 for $In_xGa_{1-x}N$ alloys [1]. The recommended values of the width and mole fraction of contact layers are shown in (Table 3).

4. Conclusions

Detailed optical analysis has been used to determine optimal structures of various designs of nitride lasers and to investigate how far these perfect designs are from their currently reported versions. In particular, recommended numbers of quantum wells in their active regions are found to be distinctly higher than values in real laser structures. Besides, those values are also much higher than the values known for conventional, i.e., arsenide and phosphide, diode lasers. Also the widths of waveguide layers have often not been properly chosen. As far as the buffer layers and the contact layers are concern, in order to preserve high Γ_{QW} and low n_{th} values, these layers should not be neither too thick nor exhibiting too high index of refraction. Some of those facts means that the current technology level of nitride laser manufacturing is still far from being optimal and/or maybe the physics of nitride lasers does not allow reaching earlier achievements of conventional arsenide and phosphide lasers.

Acknowledgements

This work was supported by the Polish State Committee for Scientific Research (KBN) as well as by the US-Poland Maria Skłodowska-Curie Joint Fund.

References

1. M.J. Bergmann and H.C. Casey, Jr., "Optical-field calculations for lossy multiple layer $Al_xGa_{1-x}N/In_xGa_{1-x}N$ laser diodes", *J. Appl. Phys.* **84**, 1196–1203 (1998).
2. T. Czyszanowski, *The application of the effective refractive index method to modelling of the electromagnetic field in heterojunction lasers* (in Polish), MSc dissertation, Technical University of Łódź, Faculty of Technical Physics, Computer Science and Applied Mathematics, 2000.
3. Y.C. Yeo, T.C. Chong, M.F. Li, and W.J. Fan, "Analysis of optical gain and threshold current density of wurtzite InGaN/GaN/AlGaN quantum well lasers", *J. Appl. Phys.* **84**, 1813–1819 (1998).
4. K. Domen, R. Soejima, A. Kuramata, K. Horino, S. Kubota, and T. Tanahashi, "Interwell inhomogenity of carrier injection in InGaN/GaN/AlGaN multiquantum well lasers", *Appl. Phys. Lett.* **73**, 2775–2777 (1998).
5. N. Tessler and G. Eisenstein, "On carrier injection and gain dynamics in quantum well lasers", *IEEE J. Quantum Electron.* **29**, 1586–1595 (1993).
6. J.F. Muth, J.D. Brown, M.A.L. Johnson, Z. Yu, R.M. Kolbas, J.W. Cook, Jr, and J.F. Schetzina, "Absorption coefficient and refractive index of GaN, AlN and AlGaN alloys", *MRS Internet J. Nitride Semicond.* **4S1**, G5.2 (1999).
7. P. Maćkowiak and W. Nakwaski, "Threshold currents of nitride vertical cavity surface-emitting lasers with various active regions", *MRS Internet J. Nitride Semicond.* **3**, 35 (1998).
8. Y. Kimura, M. Miyachi, H. Takahashi, T. Tanaka, M. Nishitsuka, A. Watanabe, H. Ota, and K. Chikuma, "Room-temperature pulsed operation of GaN-based laser diodes on a-face sapphire substrate grown by low-pressure metalorganic chemical vapour deposition", *Jpn. J. Appl. Phys.* **37**, L1231 (1998).
9. T. Czyszanowski and W. Nakwaski, "Mode transformation enhaced in nitride diode lasers by buffer layers' modification", submitted to *J. Phys. D: Appl. Phys.*
10. A. Kuramata, K. Domen, R. Soejima, K. Horino, S. Kubota, and T. Tanahashi, "InGaN laser diode grown on 6H-SiC substrate using low-pressure metal organic vapour phase epitaxy", *Jpn. J. Appl. Phys.* **36**, L1130 (1997).
11. K. Domen, A. Kuramata, R. Soejima, K. Horino, S. Kubota, and T. Tanahashi, "Lasing mechanism of InGaN-GaN-AlGaN MQW laser diode grown on SiC by low-pressure metal-organic vapour phase epitaxy", *J. Sel. Top. Quant. Electr.* **4**, 490 (1998).
12. A. Kuramata, S. Kubota, R. Soejima, K. Domen, K. Horino, P. Hacke, and T. Tanahashi, "Continuous wave operation at room temperature of InGaN laser diodes fabricated on 4H-SiC Substrate", *Jpn. J. Appl. Phys.* **38**, L481 (1999).
13. S. Nakamura, M. Senoh, S. Nagahama, N. Iwasa, T. Yamada, T. Matsushita, H. Kiyoku, Y. Sugimoto, and H. Kiyoku, "Room-temperature continuous-wave operation of InGaN multi-quantum-well structure laser diodes", *Appl. Phys. Lett.* **69**, 4056 (1996).
14. S. Nakamura, "InGaN-based blue laser diodes", *IEEE J. Sel. Top Quant. Electr.* **3**, 712 (1997).
15. S. Nakamura, M. Senoh, S. Nagahama, N. Iwasa, T. Yamada, T. Matsushita, H. Kiyoku, Y. Sugimoto, T. Kozaki, H. Umemoto, M. Sano, and K. Chocho, "High-power, long-lifetime InGaN/GaN/AlGaN-based laser diodes grown on pure GaN substrates", *Jpn. J. Appl. Phys.* **37**, L.309 (1998).
16. S. Nakamura, M. Senoh, S. Nagahama, N. Iwasa, T. Yamada, T. Matsushita, H. Kiyoku, Y. Sugimoto, T. Kozaki, H. Umemoto, M. Sano, K. Chocho, "InGaN/ /GaN/AlGaN – based laser diodes grown on GaN substrates with a fundamental transverse mode", *Jpn. J. Appl. Phys.* **37**, L.1020 (1998).
17. S. Nakamura, "InGaN multiquantum-well-structure laser diodes with GaN-AlGaN modulation-doped strained-layer superlattices", *IEEE J. Sel. Top Quant. Electr.* **4**, 483 (1998).
18. M. Miyachi, H. Ota, Y. Kimura, A. Watanabe, T. Tanaka, H. Takahashi, and K. Chikuma, "GaN-based laser diodes processed by annealing with minority-carrier injection", *Jpn. J. Appl. Phys.* **38**, L1237, (1999).

19. T. Kobayashi, F. Nakamura, K. Naganuma, T. Tojyo, H. Nakajima, T. Asatsuma, H. Kawai, and M. Ikeda, "Room--temperature continuous-wave operation of GaInN/GaN multiquantum well laser diode", *Electr. Lett.* **34**, 1494 (1998).
20. M. Kneissl, D.P. Bour, N.M. Johnson, L.T. Romano, B.S. Krusor, R. Donaldson, J. Walker, and C. Dunnrowicz, "Characterisation of AlGaInN diode lasers with mirrors from chemically assisted ion beam etching", *Appl. Phys. Lett.* **72**, 1539 (1998).
21. D.P. Bour, M. Kneissl, L.T. Romano, M.D. McCluskey, C.G. Van deWalle, B.S. Krusor, R.M. Donaldson, J. Walker, C.J. Dunnrowicz, and N.M. Johnson, "Characteristics of InGaN-AlGaN multiple-quantum-well laser diodes", *IEEE J. Sel. Top. Quant. Electr.* **4**, 498 (1998).
22. D.P. Bour, M. Kneissl, LT. Romano, R.M. Donaldson, C.J. Dunrowicz, and N.M. Johnson, "Stripe-width dependence of threshold current for gain-guided AlGaInN laser diodes", *Appl. Phys. Lett.* **74**, 404 (1999).